Solution-Phase Synthesis of Single-Crystalline Iron Phosphide Nanorods/Nanowires

Cheng Qian,[†] Franklin Kim,[‡] Lei Ma,[§] Frank Tsui,[§] Peidong Yang,[‡] and Jie Liu*,[†]

*Contribution from the Department of Chemistry, Duke University,
Durham, North Carolina 27708, Department of Chemistry, University of California,
Berkeley, California 94720, and Department of Physics and Astronomy,
University of North Carolina, Chapel Hill, North Carolina 27599*

Received September 8, 2003; E-mail: j.liu@duke.edu

Abstract: A solution-phase route for the preparation of single-crystalline iron phosphide nanorods and nanowires is reported. We have shown that the mixture of trioctylphosphine oxide (TOPO) and trioctylphosphine (TOP), which are commonly used as the solvents for semiconductor nanocrystal synthesis, is not entirely inert. In the current process, TOP, serving as phosphor source, reacts with Fe precursors to form FeP nanostructures with large aspect ratios. In addition, the experimental results show that both TOP and TOPO are necessary for the formation of FeP nanowires and their ratio appears to control the morphology of the produced FeP structures. A possible growth mechanism is discussed.

As compared to bulk materials, nanoscale materials exhibit large surface areas and size-dependent quantum confinement effects. They often have distinct electronic, optical, magnetic, chemical, and thermal properties. Recently, one-dimensional (1D) nanostructures such as wires, rods, belts, and tubes with well-controlled dimensions, composition, and crystallinity have become the focus of intensive research for investigating structure−property relationships and related scientific and technological applications due to their dimensional anisotropy.[1−3]

Significant efforts have been taken in the synthesis of various 1D nanoscale materials over the past few years. Gas-phase syntheses such as vapor−liquid−solid (VLS) methods have been successful for the preparation of various nanowires with well-controlled diameters and lengths,[3−6] especially for key semiconducting materials of groups II−VI, III−V, and IV. However, the nanowire diameters are typically larger than the strong-confinement limit, and the synthesis temperatures are generally high. The liquid/solution-phase synthesis of anisotropic nanocrystals has the potential to become a general synthetic method because it proceeds at a relatively lower reaction temperature and the diameters of the produced nanocrystals can be controlled down to several nanometers. However, as compared to the gas-phase synthesis, the liquid/solution-phase synthesis has only been demonstrated for a limited number of examples, including CdSe[7−9] and CdTe,[10] Si,[11,12] GaAs,[13−17] InAs,[18] Cu$_2$S,[19] and

metal nanowires, etc.[1,20,21] Here, we describe the use of liquid/solution-phase synthesis to prepare single-crystalline metal phosphide nanorods and nanowires with uniform diameters.

The studies on nanostructures of metal phosphides were much less advanced in comparison to other semiconductor materials because of their difficult synthetic chemistry.[22,23] Many of the bulk metal phosphide materials are technically important materials as phosphorescent, magnetic, and electronic materials.[24−26] They are important in the study of magnetism because the interatomic spacing and the anion electronegativity lie in an intermediate range between those for metals and for the oxides.[26] Traditionally, bulk iron phosphides have been prepared by a variety of high-temperature methods[25,27,28] and sonochemical

† Duke University.
‡ University of California.
§ University of North Carolina.
(1) Xia, Y. N.; Yang, P. D.; Sun, Y. G.; Wu, Y. Y.; Mayers, B.; Gates, B.; Yin, Y. D.; Kim, F.; Yan, H. O. *Adv. Mater.* **2003**, *15*, 353−389.
(2) Wang, Z. L. *Adv. Mater.* **2000**, *12*, 1295−1298.
(3) Hu, J.; Odom, T. W.; Lieber, C. M. *Acc. Chem. Res.* **1999**, *32*, 435−445.
(4) Morales, A. M.; Lieber, C. M. *Science* **1998**, *279*, 208−211.
(5) Duan, X.; Lieber, C. M. *Adv. Mater.* **2000**, *12*, 298−302.
(6) Wu, Y. Y.; Yang, P. D. *J. Am. Chem. Soc.* **2001**, *123*, 3165−3166.
(7) Peng, X. G.; Manna, L.; Yang, W. D.; Wickham, J.; Scher, E.; Kadavanich, A.; Alivisatos, A. P. *Nature* **2000**, *404*, 59−61.
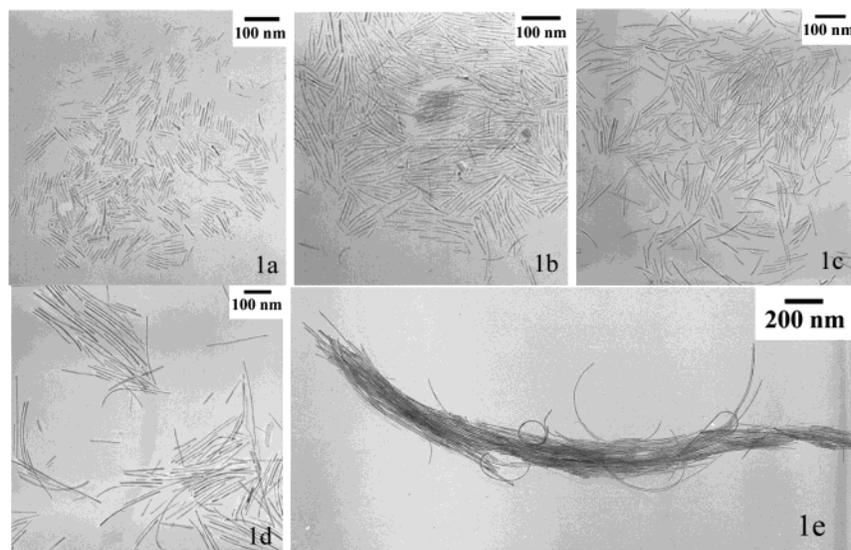
(8) Peng, Z. A.; Peng, X. G. *J. Am. Chem. Soc.* **2001**, *123*, 1389−1395.
(9) Manna, L.; Scher, E.; Alivisatos, A. P. *J. Am. Chem. Soc.* **2000**, *122*, 12700−12706.
(10) Tang, Z.; Kotov, N. A.; Giersig, M. *Science* **2002**, *297*, 237−240.
(11) Hanrath, T.; Korgel, B. A. *Adv. Mater.* **2003**, *15*, 437−440.
(12) Lu, X. M.; Hanrath, T.; Johnston, K. P.; Korgel, B. A. *Nano Lett.* **2003**, *3*, 93−99.
(13) Trentler, T. J.; Hickman, K. M.; Goel, S. C.; Viano, A. M.; Gibbons, P. C.; Buhro, W. E. *Science* **1995**, *270*, 1791−1794.
(14) Trentler, T. J.; Goel, S. C.; Hickman, K. M.; Viano, A. M.; Chiang, M. Y.; Beatty, A. M.; Gibbons, P. C.; Buhro, W. E. *J. Am. Chem. Soc.* **1997**, *119*, 2172−2181.
(15) Dingman, S. D.; Rath, N. P.; Markowitz, P. D.; Gibbons, P. C.; Buhro, W. E. *Angew. Chem., Int. Ed.* **2000**, *39*, 1470−1472.
(16) Markowitz, P. D.; Zach, M. P.; Gibbons, P. C.; Penner, R. M.; Buhro, W. E. *J. Am. Chem. Soc.* **2001**, *123*, 4502−4511.
(17) Yu, H.; Buhro, W. E. *Adv. Mater.* **2003**, *15*, 416−419.
(18) Kan, S.; Mokari, T.; Rothenberg, E.; Banin, U. *Nat. Mater.* **2003**, *2*, 155−158.
(19) Larsen, T. H.; Sigman, M.; Ghezelbash, A.; Doty, R. C.; Korgel, B. A. *J. Am. Chem. Soc.* **2003**, *125*, 5638.
(20) Wang, Y. L.; Herricks, T.; Xia, Y. M. *Nano Lett.* **2003**, *3*, 1163−1166.
(21) Sun, Y. G.; Yin, Y. D.; Mayers, B. T.; Herricks, T.; Xia, Y. N. *Chem. Mater.* **2002**, *14*, 4736−4745.
(22) Nozik, A. J.; Micic, O. I. *MRS Bull.* **1998**, *23*, 24−30.
(23) Heath, J. R.; Shiang, J. J. *Chem. Soc. Rev.* **1998**, *27*, 65−71.
(24) Arinsson, B.; Landstrom, T.; Rundquist, S. *Borides, Silicides and Phosphides*; Wiley: New York, 1965.
(25) Greenwood, N. N.; Earnshaw, A. *Chemistry of the Elements*; Pergamon Press: New York, 1994; pp 563−564.
(26) Stein, B. F.; Walmsley, R. H. *Phys. Rev. B* **1966**, *148*, 933−939.

Figure 1. TEM images of FeP nanowires prepared in 50 wt % TOPO in TOP via (a) single injection and multiple injections (b, 2 times; c, 3 times; d, 6 times; and e, 15 times).

methods.[29] Ultrafine powder of iron phosphides was also synthesized by a solvothermal method,[30] but the morphology is ill-defined and the average particle size was large (~200 nm in diameter). Over the last year, the preparation of nanostructured metal phosphides has gained significant interest due to the need to explore the size-dependent physical properties in these materials. Nanoparticles of Fe_2P, FeP, and other metal phosphides have been prepared recently.[31,32] However, the diameters of the produced nanoparticles are not uniform. Additionally, to the best of our knowledge, high-quality and uniform iron phosphide nanorods and nanowires have never been prepared.

In this paper, we report a novel one-step solution-phase route to prepare iron phosphide nanorods and nanowires. Our experiments have used a mixed solvent (trioctylphosphine oxide (TOPO) and trioctylphosphine (TOP)) that is commonly used by many groups for the preparation of various nanostructures. We have shown here that TOP may react with Fe precursors and act as P source for the formation of iron phosphide nanostructures rather than behaving as inert solvent in previous experiments.

In a typical experiment, 5 g of TOPO (99% from Aldrich) and 6 mL of TOP (97% from Aldrich) were mixed as initial solvent (TOPO in TOP of 50 wt %) and then heated to a desired temperature (>300 °C) with vigorous stirring under N_2 atmosphere. Next, 0.5 mL of stock solution 1 (made from 1 mL of $Fe(CO)_5$ dissolving in 4 mL of TOP) was quickly injected into this rapidly stirred, hot TOPO/TOP solution. The temperature dropped to about 300 °C after the injection. The temperature was kept constant at 300 °C for further growth. At each 30 min interval, a 0.2 mL portion of liquid was extracted from the reaction solution to monitor the growth process, and 0.2 mL of

stock solution 1 was injected to keep the total volume unchanged. The removed liquid was dispersed in hexane. A drop of this solution was deposited on a copper TEM grid and checked under a transmission electron microscope (TEM).

Figure 1 shows TEM images of the prepared nanorods and nanowires as a function of reaction time. As shown in the figures, nanorods and nanowires with uniform diameter of about 5 nm can be prepared. Interestingly, the length of the nanorods increases as a function of reaction time, while the diameter remains essentially unchanged. Nanowires with length up to a few microns (aspect ratio >200) can be prepared by the multiple injections method (Figure 1e).

Energy-dispersive X-ray spectroscopy (EDX) analysis of the nanowires showed that Fe and P were the main elemental components (Figure 2a). Quantitative EDX analysis showed the mole ratio of Fe:P was in the range of 1:1 to 1:1.5. Analysis of these nanowires using XPS further confirms the observation. Oxygen and carbon were also found in the XPS spectrum, which could come from surface adsorption of oxygen and carbon dioxide.[33] Another source of the oxygen and carbon signals could be the surfactant TOPO that was not completely removed by the surface-cleaning step. To reduce the effect of surface adsorption, we used an ion gun to etch the surface of our samples for 10 and 20 min to remove approximately 1 and 2 nm of the surface layer. The resulting binding energy changes were shown in Table 1. There were slight chemical shifts between the Fe and P on the surface and those in the inner part of the nanowires. From the binding energy of Fe and P on the surface, we can exclude the possibility of any type of iron oxides and phosphates formation, which should have binding energies larger than 709 and 130 eV, respectively.[33]

All peaks in the X-ray diffraction (XRD) pattern (Figure 2b) can be indexed to the orthorhombic cell of the FeP phase with space group *Pnma* (lattice constant $a = 5.191$ Å, $b = 3.099$ Å, and $c = 5.792$ Å).[34] High-resolution TEM images and electron

(27) Corbridge, D. E. C. *Phosphorus, An Outline of its Chemistry, biochemistry and Technology*, 5th ed.; Elsevier: New York, 1995.
(28) Fitzmaurice, J. C.; Hector, A. L.; Parkin, I. P. *J. Mater. Sci. Lett.* **1994**, *13*, 1−2.
(29) Sweet, J. D.; Casadonte, D. J. *Ultrason. Sonochem.* **2001**, *8*, 97−101.
(30) Gu, Y. L.; Guo, F.; Qian, Y. T.; Zheng, H. G.; Yang, Z. P. *Mater. Res. Bull.* **2002**, *37*, 1101−1105.
(31) Stamm, K. L.; Gamo, J. C.; Liu, G. Y.; Brock, S. L. *J. Am. Chem. Soc.* **2003**, *125*, 4038−4039.
(32) Lukehart, C. M.; Milne, S. B.; Stock, S. R.; Shull, R. D.; Wittig, J. E. *Nanotechnology* **1996**, *622*, 195−204.

(33) Moulder, J. F.; Stickle, W. F.; Sobol, P. E.; Bomben, K. D. *Handbook of X-ray Photoelectron Spectroscopy: A Reference Book of Standard Spectra for Identification and Interpretation of Xps Data*; Perkin-Elmer: Boston, 1995.
(34) Rundqvist, S. *Acta Chem. Scand.* **1962**, *16*, 287−292.
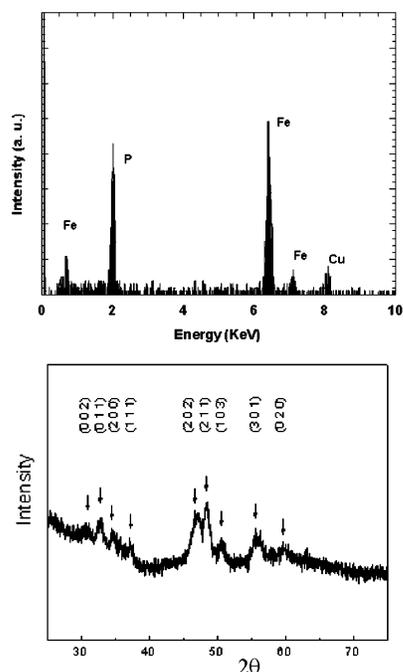
Figure 2. (a) Energy-dispersive X-ray spectroscopy (EDX) of FeP nanowires. The Cu signal is from copper TEM grid. (b) XRD pattern of FeP nanowires. All peaks can be indexed according to the orthorhombic structure of FeP.

Table 1. Binding Energy (BE) of Fe and P in FeP Nanowires

	surface	10 min spattering	20 min spattering
Fe 2p	707.3 eV	707.0 eV	707.0 eV
P 2p	129.1 eV	128.8 eV	128.8 eV

diffraction pattern further confirmed that the produced nanowires were single-crystalline FeP nanowires. The electron diffraction pattern (Figure 3a) was taken on bundles of the FeP nanowires. Ring diffractions with *d* values of 2.740, 2.427, 1.993, 1.879, 1.754, 1.624, and 1.536 Å can be identified as (011), (111), (112), (211), (301), (212), and (020) peaks from the FeP orthorhombic structure, respectively. A weak diffraction at 2.207 Å cannot be identified using the FeP structure, presumably from either Fe or Fe_2P impurities. High-resolution TEM (Figure 3b,c) studies indicate most of these nanowires grow perpendicular to either (011) or (013) planes. In addition, the wires are usually covered with a thin layer of amorphous coating.

Consistent with the HRTEM results, XPS analysis results also indicated that the surfaces of FeP nanowires were possibly coated with the surfactant TOPO, or some other unknown amorphous Fe−P compounds. Moreover, the quantitative EDX analysis also showed the mole ratio of FeP was in the range of 1:1 to 1:1.5, which also proved that the nanowires were mainly FeP; the excess amount of P should come from the amorphous layer on the surface, most likely the surfactants.

To understand the formation mechanism of these nanowires and identify the source of phosphor, we have performed a series of experiments. We have first excluded the possibility that the phosphor source was the impurities in TOPO and TOP because the amount of phosphor in the products far exceeds the amount of impurity in the solvents. We have then found that such nanostructures can only be prepared in the presence of TOP. When pure TOPO was used, only spherical Fe nanoparticles were prepared under identical reaction conditions (Figure 4a).
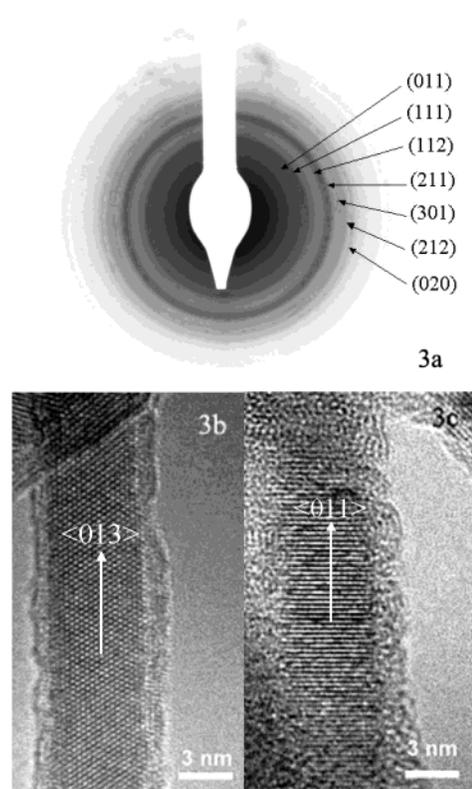
Figure 3. Electron diffraction pattern (a) and HRTEM images of FeP nanowires (b, c). The nanowires grow perpendicular to (013) and (011) planes in b, c, respectively.

Obviously, the TOP in the mixture not only functions as a cosolvent but also as the P sources in our experiments. As reported previously, a variety of phosphine-substituted iron carbonyl intermediate species could form when $Fe(CO)_5$ is dissolved in TOP.[29] We assume that after being injected into hot TOPO/TOP solutions at high temperature, these intermediate species could decompose to produce FeP by cleaving the Fe−C and P−C bonds. The process could be simply described as follows:

$$Fe(CO)_5 + TOP \rightarrow (CO)_xFe(P(C_8H_{17})_3)_y + heat \rightarrow FeP$$
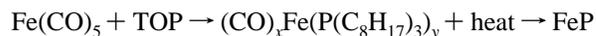
Multiple injection of stock solution provided feedstocks for further growth of FeP structures. However, to grow long and uniform nanowires, the ratio between TOP and TOPO is very important. Although FeP nanorods can prepared without TOPO (Figure 4b), the diameter distribution is much broader and the aspect ratio is lower. At higher TOPO concentration, although the diameters are uniform, the lengths are usually only tens of nanometers (Figure 4c). The optimal ratio of TOPO/TOP is about 50% (Figure 1) to obtain uniform nanorods and nanowires.

Several recent studies have given some insight into the shape control of anisotropic nanocrystals.[1,35] It is well accepted that the existence of an appropriate amount of capping reagents can alter the surface energies of various crystallographic surfaces to promote selective anisotropic growth of nanocrystals. In our cases, we believe TOPO played the role of the capping reagent because the morphology of the produced nanowires is greatly affected by its concentration. From the experimental results,

(35) Lee, S. M.; Cho, S. N.; Cheon, J. W. *Adv. Mater.* **2003**, *15*, 441−444.
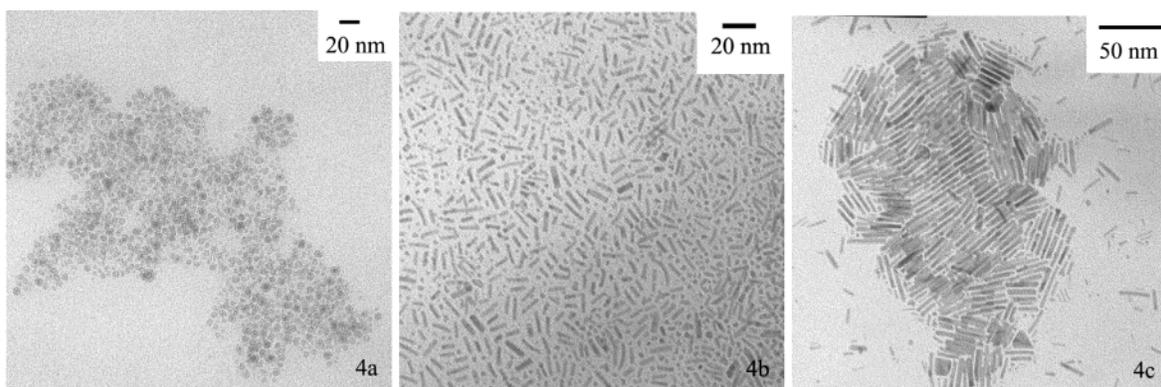
Figure 4. TEM images of nanocrystals prepared in TOPO (a), TOP (b), and 90 wt % TOPO in TOP (c).
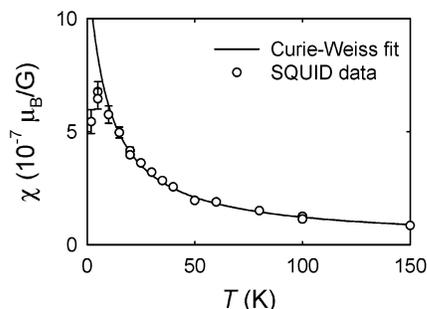
Figure 5. Magnetic susceptibility χ ($\equiv \partial M/\partial B$) of FeP nanowires at $B \approx 2$ T as a function of temperature. Circles are measurements using SQUID magnetometry. The line is a Curie–Weiss law fit of the data with a Curie constant of $(1.1 \pm 0.1) \times 10^{-5}$ μ_B-K/G and Curie–Weiss temperature of -9 ± 1 K. The former corresponds to an effective polarization of 0.7 μB per Fe, and the latter indicates the presence of antiferromagnetic interactions.

TOPO molecules absorbed on the FeP nanocrystals greatly increased the growth rate along the direction perpendicular to (011) and/or (013) planes of the FeP structure relative to all other crystal planes. The concentration of TOPO in our system is very important for causing a large difference among the growth rates of various crystallographic surfaces. Additionally, TOPO was shown to play a very important role in promoting atomic exchange between nanoparticles, a requirement for size distribution focusing and kinetic control.[36] A similar effect may also exist in our system. TOP in the mixture reacts with $Fe(CO)_5$ for the formation of FeP. Without TOPO, the produced nanocrystals were a mixture of nanorods and nanoparticles.

Magnetic properties of the FeP nanowire have been studied using SQUID magnetometry in a temperature range between 2 and 400 K and a field range up to 5 T. Bulk FeP exhibits a double helical magnetic structure propagating along the *c*-axis below a Néel temperature T_N of 115 K.[37,38] The helimagnetic structure consists of two types of Fe sites with respective magnetic moments of 0.46 and 0.37 μ_B. This ordering is suppressed in the nanowires. As shown in Figure 5, the differential magnetic susceptibility χ of the nanowire powder, defined as $\partial M/\partial B$, exhibits a Curie–Weiss paramagnetism down to 10 K with

$$\chi = C/(T - \theta) \qquad (1)$$

where C is the Curie constant and θ is the Curie–Weiss temperature. At lower temperatures, it deviates from the Curie–Weiss law and rises to a peak around 5 K. The respective

paramagnetic parameters obtained from the fits of the behavior at fields above 0.1 T are $(1.1 \pm 0.2) \times 10^{-5}$ μ_B-K/G per Fe and -10 ± 2 K. The measured Curie constant for Fe corresponds to an effective magnetic moment of 0.7 ± 0.2 μ_B, which is consistent with the bulk value but nearly a factor of 10 smaller than the values for free Fe spins. The negative Curie–Weiss temperature indicates the presence of antiferromagnetic interactions, and the low-temperature peak of χ further suggests the presence of antiferromagnetic correlation. The observed magnetic behavior appears to be independent of the morphology of the nanostructures. However, the low-field signal from the nanowires is not detectable, because of the presence of a small quantity of unknown ferromagnetic clusters (possibly Fe or Fe_2P, <0.1 wt %) in the powder with a T_C of ~270 K, so more quantitative interpretation of possible ordering is not possible, which would require quantitative measurements of the behavior at very low fields (≪0.1 T).

In summary, high-quality FeP nanorods/nanowires have been synthesized in the TOPO/TOP solvent systems via a simple one-step solution-phase route. The length of the nanorodes/nanowires can be continuously increased by a multiple injection method. Unlike previous reports of nanostructure synthesis in the TOP/TOPO system, TOP acts as both solvent and phosphor source in our experiment. Interestingly, a recent article also reported that under the right conditions, dodecanethiol, which is typically used as a capping ligand, can function as a sulfur source for nanorod synthesis.[19] These findings showed that we need to be very careful in selecting the solvent and capping agents in nanoparticle and nanowire synthesis. Inert solvent and capping ligands for one reaction may be reactive for a similar but different reaction. Additionally, the produced FeP nanowires exhibit paramagnetism down to 10 K, below which the presence of antiferromagnetic correlations was observed.

(36) Puntes, V. F.; Krishnan, K. M.; Alivisatos, A. P. *Science* **2001**, *291*, 2115–2117.
(37) Felcher, G. P.; Smith, F. A.; Bellavance, D.; Wold, A. *Phys. Rev. B* **1971**, *3*, 3046.
(38) Häggström, L.; Narayanasamy, A. *J. Magn. Magn. Mater.* **1982**, *30*, 249.